Dual-Gate Silicon Carbide (SiC) Lateral Nanoelectromechanical Switches

Tina He†, Rui Yang, Srihari Rajgopal, Swarup Bhunia, Mehran Mehregany, Philip X.-L. Feng†
Electrical Engineering, Case Western Reserve University, Cleveland, OH 44106, USA
†Email: ting.he@case.edu; philip.feng@case.edu

***Abstract*—We present demonstration and experimental results of four-terminal nanoscale electromechanical switches with a novel dual-gate design in a lateral configuration based on polycrystalline silicon carbide (poly-SiC) nanocantilevers. The switches operate at both room temperature and high temperature up to $T \approx 500^{o}$C in ambient air with enhanced control over the *distributed* electrostatic actuation force, and also enable recovery from stiction at contact. We have experimentally demonstrated multiple switching cycles of these nanomechanical switches with different actuation control schemes, and active release from stiction by exploiting a repulsive mechanism. In combination with modeling of cantilever deflection, the experiments help reveal the coupled electromechanical behavior of the device when making contact during switching operations, and suggest possible correlation between the switch degradation observed over cycles and the elastic deformation of nanocantilevers.**

Keywords—Nanoelectromechanical Systems (NEMS); Silicon Carbide (SiC); Switches; Dual-Gate; High Termperature

I. INTRODUCTION

Contact-mode mechanical switches (relays) miniaturized down to the truly nanometer scale, enabled by the emerging nanoelectromechanical systems (NEMS), are being actively studied as an alternative to the currently dominating CMOS transistor switches for future ultra-low-power applications [1-6]. NEMS switches offer abrupt switching characteristics and minimal off-state leakage. Beyond NEMS switches based on state-of-the-art silicon-on-insulator (SOI) technology [5], silicon carbide (SiC) has outstanding mechanical, chemical and thermal properties and thus enables operations at high temperature and in harsh environments, while also being compatible with Si, SiO_2, and SOI substrates in mainstream microelectronics. Three-terminal SiC NEMS switches with single-gate structure have been demonstrated with robust long-cycle operations at room temperature and high temperature [6]. A central challenge in all NEMS switches (including SiC) is on the nanoscale contacts. Schemes and readout techniques that may help study the contact evolution and even help control the contact mechanism, toward avoiding stiction or other contact-related failure modes, are highly desirable.

In this work, we attempt a novel design of a four-terminal, dual-gate NEMS switch to explore the possibility of improved control of electromechanical actuation for enhancement of switching dynamics and contact. By splitting the conventional single gate into two or more local gates, one expects to have more control of the electrostatic force. We also attempt to recover devices suffering from contact stiction by exploiting charge repulsion between the cantilever beam and gate/drain.

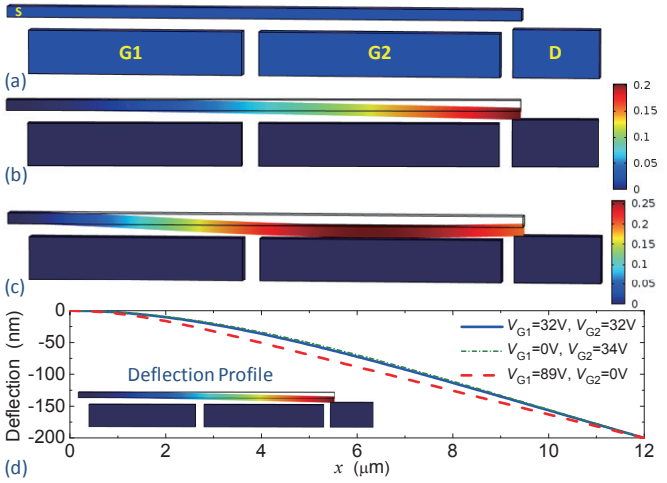

Figure 1. Finite element modeling (FEM, based on COMSOL) of the cantilever beam deflection with double gate electrodes. (a), (b), (c) Deflection profile of the beam when both G1 and G2 are biased at (a) 0V, (b) 32V, and (c) 130V, showing (a) no deflection, (b) beam just contacting the drain (D), and (c) beam bending toward G2 after touching the drain. (d) Comparison of the deflection profiles when the beam is just contacting the drain under various gate voltages on G1 and G2, with x in the beam length direction.

In conceptual design as illustrated in Fig. 1, more control of the electrostatic actuation can be achieved by applying different combinations of voltages on the two local gates while monitoring the currents. Figure 1a illustrates the idea of this new configuration with finite element modeling (FEM, in COMSOL), where G1 and G2 denote the two local gates. Since these gates can have various dimensions, locations, and applied voltages (V_{Gi}, i is the gate index), it becomes possible to engineer the '*pattern*' of the actuation forces, and therefore to gain control of switching dynamics and contact mechanics of the NEMS switches. Figure 1b & 1c show COMSOL simulation results of the deflected cantilever profile when both G1 and G2 are connected together as one single gate, with a varying but common actuation voltage. Figure 1d shows the cantilever deflection profile when G1 and G2 are connected separately, and with different applied gate voltages.

II. NANOFABRICATION OF SiC NEMS

The SiC NEMS devices in this work are enabled by a poly-SiC-on-SiO_2 technology. The device structural layer is a 500nm-thick polycrystalline SiC (poly-SiC) film grown at

900°C on 500nm SiO_2 on Si substrate (4-inch wafer), by using low-pressure chemical vapor deposition (LPCVD). All designed features (from NEMS structures to electrodes and pads) are patterned by employing high-resolution wafer-scale electron-beam lithography (EBL). Reactive ion etch (RIE) is used to transfer patterns to the SiC device layer. Devices are finally released by etching the exposed SiO_2 in vapor HF. The detailed nanofabrication process is illustrated in Ref. [6].

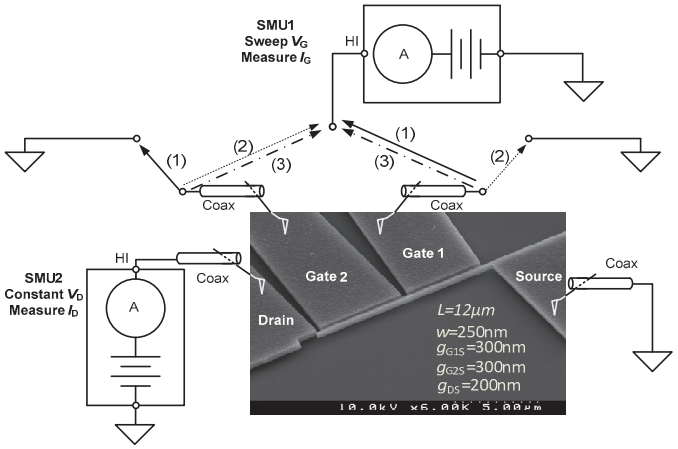

Figure 2. DC measurement schemes for testing the dual-gate SiC NEMS switches. Each gate can be connected as one of the following: not connected, connected to an SMU to sweep the voltage, and connected to an SMU with a constant voltage supply. This forms 3 connection schemes: **(1)** Disconnect G2 and use only G1 to actuate by sweeping the voltage. **(2)** Disconnect G1 and use only G2 to actuate. **(3)** Connect G1 & G2 together as one gate with a common sweeping voltage. All cables are tri-axial except labeled 'coax'.

III. *I-V* Characteristics in Ambient Air

A. Experimental Setup & Measurement Schemes

Figure 2 shows the scanning electron microscopy (SEM) image of a typical dual-gate switch, embedded in a DC measurement setup. We employ two high-precision source measurement units (SMUs) to carefully measure the *I-V* characteristics of the dual-gate NEMS switches with three different gate connection schemes. Scheme (1) is to connect SMU1 to G1 and sweep only gate voltage on G1 from 0V to the actuation voltage, V_G, and then back to 0V, at the same time measure the gate-to-source current I_G. Scheme (2) is the same as scheme (1) except only G2 is connected to sweep the voltage. Scheme (3) is to connect both G1 and G2 together as one gate to actuate the switch. In all of the three schemes the source is connected to ground and another SMU is connected to the drain to define a bias voltage and measure the current from drain to source I_D. By carefully measuring I_D and I_G we monitor drain-source (D-S) conduction, possible/unwanted gate-source (G-S) leakage, *I-V* hysteresis (very typical for NEMS [6]), as well as all the possible contacts upon actuation controlled by applying and sweeping the gate voltages.

B. Characteristics with Connection Schemes (1) & (2)

Figure 3 shows the NEMS switch turning on and off with connection scheme (1) (actuated by G1 alone), at V_{on}=13.6V and V_{off}=5.6V, respectively. The on-state current is I_{on}≈20nA. After this, by measuring the current between G1 and G2, shown in the inset of Fig. 3b, we have also confirmed that G1 and G2 are still electrically isolated. This verifies that we have independent control of the gate actuation on each gate.

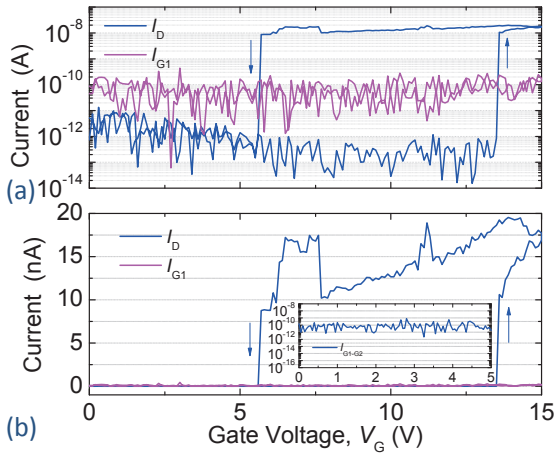

Figure 3. *I-V* characteristics of the switching in connection scheme **(1)** – using only G1 to actuate, with measured currents in (a) semi-logarithmic scale and (b) linear scale. Inset of (b) shows the control measurement between G1 and G2, which confirms that the two gates are not shorted.

Figure 4 displays the measured switching on and off events for two cycles taken immediately after the above tests, under the control of G2 only. The first cycle has a switch-on voltage V_{on}=13.5V and switch-off voltage V_{off}=6.3V, with on-state current I_{on}≈1nA. The second cycle has V_{on}=13.6V and V_{off}=6.2V, with on-state current I_{on}≈2nA.

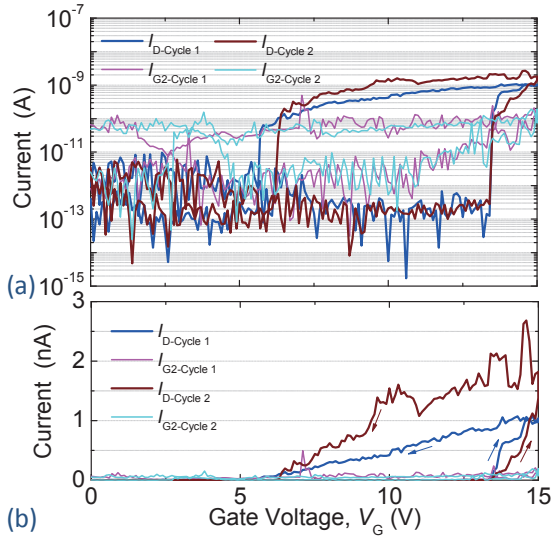

Figure 4. *I-V* characteristics of the switching in connection scheme **(2)** – using only G2 to actuate, tested for two consecutive cycles, with data shown in (a) semi-logarithmic scale and (b) linear scale, respectively.

These results demonstrate that the dual-gate SiC NEMS switch can be actuated using either of the two local gates, with similar switch-on and switch-off voltages, although switching on and off using G1 appears much more abrupt than using G2. We also notice that the on-state current obtained in scheme (1) is much higher than that in scheme (2). Multiple effects may

have contributed to the observed differences in the switching characteristics. It can be inferred that the change in location of the actuating gate (G1 *vs* G2) leads to the change in electrostatic force and its effective region on the beam, which results in the change in the abruptness in *I-V* characteristics and actual contact details. A second possible effect might be that during the first contact the beam could have experienced a permanent shape change due to bending and deformation upon contact. Another effect might be the nanocontact degrading during "hot" switching operation, which has been observed in very recent work on poly-SiC NEMS switches [6].

C. Connection Scheme (3) & Recovery from Stiction

Figures 5a & 5b show the *I-V* curves of the SiC NEMS switch using both G1 and G2 to actuate, as in scheme (3) shown in Fig. 2. Measured I_D curve clearly indicates that the (S-D) contact gets in stiction after this switching event, and does not release even when $V_{G1,2}$ decreases to 0V. The I_G curve also suggests increasing gate-to-source (G1&2-S) leakage. The stiction occurs when the contact adhesion force is larger than the NEMS restoring force, which could be a very frequent failure mechanism in NEMS switches.

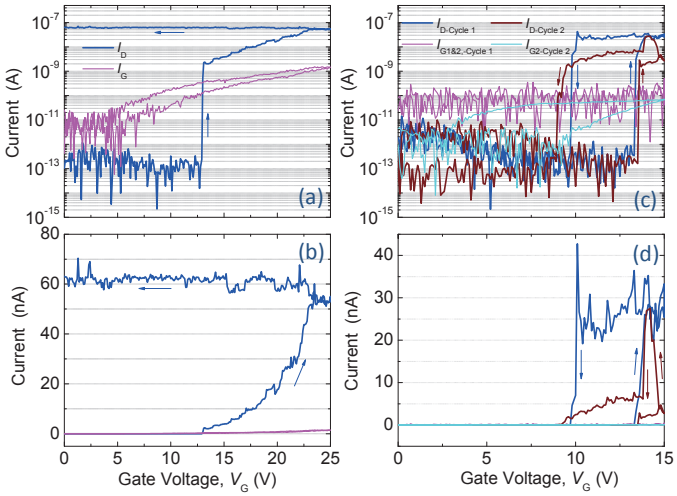

Figure 5. Measured *I-V* curves of the dual-gate NEMS in connection scheme **(3)** – connecting both G1 and G2 together for actuation, with data shown in (a) semi-logarithmic scale and (b) linear scale for the very first switching attempt. (c) & (d) *I-V* curves of two consecutive cycles of switching tested after the recovery from stiction. Cycle 1: the same test as performed in (a) & (b) (connection scheme **(3)** – V_{G1}=V_{G2}). Cycle 2: another test in connection scheme **(2)** – using only G2 to actuate.

Cantilever beams in stiction with contacts could be non-trivial to recover. We have considered and explored multiple possibilities and schemes, such as (i) NEMS designs including complementary gates to allow active pull-off by an 'image' gate (with respect to the initial actuation gate) on the opposite side of the movable cantilever/beam [3,5], (ii) exploiting the repulsion between charges of the same polarity (as in the famous Coulomb's experiments back in 1785). In this work we do not have complementary gates fabricated for pull-off actuation upon cantilever tip stiction at contact. We have attempted and made successful trails with the charge repulsion to recover and salvage devices from contact stiction. We note here that exploiting charge repulsion to actively separate and recover nanostructures from contact stiction (due to adhesion arising from interfacial van der Waals forces) has earlier been explored and demonstrated in contact-mode carbon nanotube electromechanical tweezers and switches [1,7].

Immediately after the test switching cycle shown in Fig. 5a & 5b, we apply an exactly same voltage onto the gate 1 (G1) and the NEMS cantilever, including both the drain (D) and the source (S) simultaneously (where D and S are shorted together after the first switching cycle, see Fig. 5a & 5b); and we sweep this voltage from 0V up to 25V. Here the key is to keep the voltage exactly the same, to ensure there is no voltage drop between the terminals to be separated by repulsion between the built charges of the same polarity.

To examine the effectiveness of this device recovery attempt, we immediately perform a measurement with connection scheme (3), and the measured *I-V* characteristics are shown as the first switching cycle plotted in Fig. 5c & 5d. This clearly shows excellent NEMS switching behavior with V_{on}≈13.4V, V_{on}≈9.7V, and I_{on}≈20–40nA, with $I_{on}/I_{off}>10^4$. In comparison with the data in Fig. 5a & 5b before the repulsion testing, clearly the device has recovered, and the S-D contact stiction issue is not persistent.

We then follow on to perform another switching cycle with measurement connection scheme (2), with the measured data plotted as the second cycle data in Fig. 5c & 5d. This again clearly confirms that the stuck cantilever beam has already been successfully recovered, and is able to switch much better than the very first cycle (Fig. 5a & 5b). Nonetheless, here in Fig. 5c & 5d, measured 'Cycle 1' switching characteristics (in connection scheme (3)) seem to be better than the behavior measured in 'Cycle 2' (in connection scheme (2)).

TABLE I. *I-V* CHARACTERISTICS BEFORE AND AFTER RECOVERY

Connection & Test Scheme	Before Recovery			After Recovery		
	V_{on}	V_{off}	I_{on}	V_{on}	V_{off}	I_{on}
(2) (Gate 2 Only)	13.6V	6.3V	2nA	13.6V	9.5V	20nA
(3) (Gate 1 & 2)	13.1V	–	3nA	13.4V	9.7V	30nA

In order to examine the nanoscale contact in the dual-gate switch operations, in Table I we compare the switch-on voltage V_{on}, switch-off voltage V_{off}, and on-state current I_{on} of the same device, which are measured immediately before and after the repulsion test for recovery from stiction. We find that for the same connection scheme, the switch-on voltage V_{on} does not change much, but switch-off voltage V_{off} and on-state current I_{on} increase quite considerably, after the stiction and recovery. Increased V_{off} values clearly suggest less adhesion energy (less hysteresis in the switching curve); and higher I_{on} means a much better contact.

We notice that the gate current in the last cycle as shown in Fig. 5c & 5d increases with increasing gate voltage, which indicates the cantilever might have made contact with both D

and G2 when the device switches on. One possible scenario could be that the cantilever beam has slightly bent toward G2 instead of being as straight as in the original shape. We note that in this case G1/G2, D and S are not shorted together.

To reduce the observed $I_{G\text{-}Cycle2}$ shown in Fig. 5c & 5d, and based on the above reasoning, we attempt to actively push the cantilever beam further away from G2, by applying voltage of same polarity to both S and G1/G2 (connected together), and sweep the voltage from 0V to 25V.

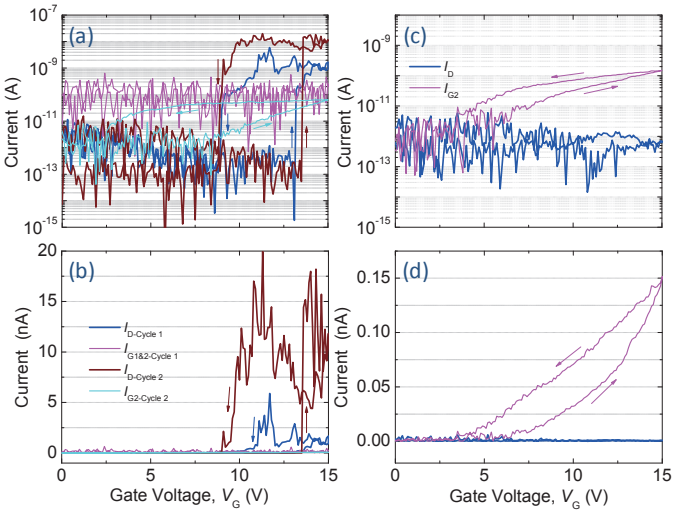

Figure 6. (a) & (b) *I-V* characteristics of two new cycles of switching tested after testing shown in Fig. 5c & 5d and G1/G2-S repulsion test. Cycle 1: connection scheme **(3)** with both G1 & G2 for actuation. Cycle 2: connection scheme **(2)** with only G2 for actuation. (c) & (d) *I-V* curves of the last switching cycle tested showing certain gate leakage (G2-S) but no clear contact-mode mechanical switching from S to D.

We repeat the switching tests with connection schemes (3) and (2) after the above repulsion attempt. Measured *I-V* curves in Fig. 6a & 6b show that when we actuate the switch with both G1 and G2 at the same time as shown in cycle 1, the gate current I_G shows no leakage between G1/G2 and S. But in data from cycle 2, in which we actuate the NEMS switch with G2 alone (in connection scheme (2)), G2 would partially contact S when the device switches on. The results suggest that switches design with G2 only might have a higher chance to fail due to G2-S stiction. Later, as we attempt more cycles with only G2 actuation (scheme (2)), the obtained data in Fig. 6c & 6d exhibit no contact-mode switching between S and D, but suggests a partial contact between G2 and S. This behavior might have resulted from a deformation of the relatively long device (L=12μm), with its profile being more like in Fig. 1c rather than in Fig. 1b (the preferred situation).

IV. High Temperature Operation

Poly-SiC NEMS also have outstanding thermal, mechanical properties that enable switching operation at high temperature (up to T≈500°C) [4,6]. Figure 7 shows another dual-gate SiC NEMS switch operating at high temperature in air. In this experiment we apply a constant voltage V_{G2}=5V to G2, and sweep the voltage on G1 from 0V to 10V. The data shows a low switch-on voltage V_{on}≈3.0V, with minimal $I_{G1,G2}$ which are within the off-state leakage levels of the system at 500°C (higher than that at room temperature, as connections and cables needed are different). The measured I_{on} should be >100nA, which is the current limit set for this measurement. The noticeable leakage ($I_{D,off}$) is non-intrinsic to the NEMS.

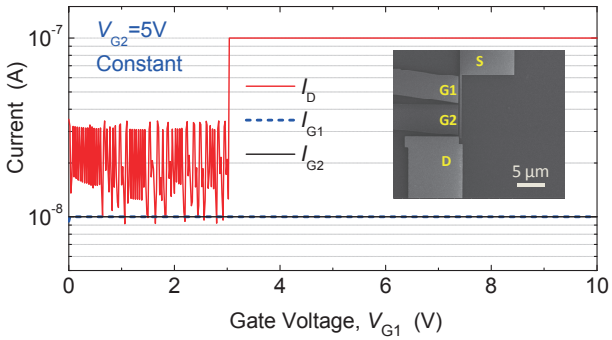

Figure 7. Measured *I-V* characteristics of a dual-gate SiC NEMS switch at T≈500°C, clearly showing an abrupt switching event at V_{on}≈3.0V. The inset shows an SEM image of the specific dual-gate SiC NEMS switch device.

V. Conclusion

We have demonstrated a new type of poly-SiC lateral NEMS switches with a dual-gate design that allows for studying control of electrostatic actuation by two local gates, and opens the possibility toward exploring more flexible control via multiple distributed gates. Prototype switches are demonstrated to operate at both room and high (T≈500°C) temperatures. The design also provides a means for gaining more information on nanocontacts and switching dynamics. Future designs with optimized device dimensions and number of distributed local gates are expected to further improve the performance and control of switching dynamics and contacts.

Acknowledgment

We thank the financial support from DARPA MTO (NEMS Program, D11AP00292) & NSF (CCF-1116102).

References

[1] T. Rueckes, K. Kim, E. Joselevich, G.Y. Tseng, C.-L. Cheung, C.M. Lieber, "Carbon nanotube-based nonvolatile random access memory for molecular computing," *Science*, vol. 289, pp. 94-97, Jul. 2000.

[2] M.L. Roukes, "Mechanical computation, redux?" in *Tech. Digest, IEEE International Electron Devices Meeting (IEDM 2004),* pp. 539-542, San Francisco, CA, Dec. 13-15, 2004.

[3] X.L. Feng, M.H. Matheny, C.A. Zorman, M. Mehregany, M.L. Roukes, "Low voltage nanoelectromechanical switches based on silicon carbide nanowires," *Nano Letters*, vol. 10, pp. 2891-2896, Aug. 2010.

[4] T.-H. Lee, S. Bhunia, M. Mehregany, "Electromechanical computing at 500°C with SiC," *Science*, vol. 329, pp. 1316-1318, Sep. 2010.

[5] R. Yang, T. He, C. Marcoux, P. Andreucci, L. Duraffourg, P.X.-L. Feng, "Silicon nanowire and cantilever electromechanical switches with integrated piezoresistive transducers," in *Proc. 26th IEEE Int. Conf. on Micro Electro Mechanical Systems* (*MEMS 2013*), pp. 229-232, Taipei, Taiwan, Jan. 20-24, 2013.

[6] T. He, R. Yang, S. Rajgopal, M.A. Tupta, S. Bhunia, M. Mehregany, P. X.-L. Feng, "Robust silicon carbide (SiC) nanoelectromechanical switches with long cycles in ambient and high temperature conditions," in *Proc. 26th IEEE Int. Conf. on Micro Electro Mechanical Systems* (*MEMS 2013*), pp. 516-519, Taipei, Taiwan, Jan. 20-24, 2013.

[7] P. Kim, C.M. Lieber, "Nanotube nanotweezers," *Science*, vol. 286, pp. 2148-2150, Dec. 1999.